



Investigation of modified *Ginkgo biloba* leaves extract as eco-friendly inhibitor for the corrosion of N80 steel in 5% HCl

Xuefan Gu^a, Ke Dong^a, Jing Tian^a, Hong Li^a, Jie Zhang^a, Chentun Qu^{a,b,c,*}, Gang Chen^{a,b,c,*}

^aCollege of Chemistry and Chemical Engineering, Xi'an Shiyou University, Xi'an Shannxi 710065, China, email: xuefangu@xsyu.edu.cn (X. Gu), theonlymannba1988@163.com (K. Dong), 343498114@qq.com (J. Tian), 841911637@qq.com (H. Li), zhangjie@xsyu.edu.cn (J. Zhang)

^bState Key Laboratory of Petroleum Pollution Control, CNPC Research Institute of Safety and Environmental Technology, Beijing, 102206, China

^cShaanxi Province Key Laboratory of Environmental Pollution Control and Reservoir Protection Technology of Oilfields, Xi'an Shaanxi, 710065, China, email: xianquct@xsyu.edu.cn (C. Qu), gangchen@xsyu.edu.cn (G. Chen)

Received 17 September 2017; Accepted 28 February 2018

ABSTRACT

Extract of *Ginkgo biloba* was modified with Mannich reaction to produce the relative stable green acidic corrosion inhibitors. The inhibition of *Ginkgo biloba* leaves extract (GLE) and the derivatives (MGLEs) as green and eco-friendly corrosion inhibitors on corrosion of N80 steel in 5% HCl solution was studied by methods of polarization curves, scanning electron micro graph (SEM) and weight loss. The results showed that the GLE and MGLEs are effective for corrosion inhibition, and the MGLEs are more potent than that of GLE. The inhibitor molecules adsorb on the metal surface following a Langmuir adsorption isotherm. They offered good inhibition for mild steel and act as mixed inhibitors. The surface topography of the steels before and after being corrupted showed that the extracts offer good protection. In addition, both GLE and MGLEs are active against sulfate reducing bacteria (SRB), iron bacteria (IB) and total general bacteria (TGB).

Keywords: *Ginkgo biloba*; Extract; Mannich reaction; Acidification; Micro biologically influenced corrosion

1. Introduction

Corrosion is defined as the degradation of a material due to a reaction with its environment. This can be a weakening of the material due to a loss of cross-sectional area, it can be the shattering of a metal due to hydrogen embrittlement, or it can be the cracking of a polymer due to sunlight exposure [1]. In oilfield, to enhance oil recovery, acidification is one of the efficient operations in oilfield, during which hydrochloric acidic fluid is pumped into wells to enlarge the permeability. However, acidizing can cause serious metal corrosion and lead to great economic losses and security risks [2,3]. As it is a great threat for the metal instruments involved in the acidification, there is a need to smooth these negative effects

away. Therefore, for the oil industry, adding inhibitor into acid fluid during acidizing treatment is considered as the most common and effective way against such acid attack [3,4]. According to the literatures, the organic compounds, containing heteroatoms, such as sulfur, phosphorus, nitrogen and oxygen, together with aromatic rings, are efficient as corrosion inhibitors [5].

Although many compounds have been synthesized for the corrosion inhibition, there is a need to develop green and eco-friendly corrosion inhibitors with the increased awareness of environmental protection and sustainable development of society. Extracting effective components from natural plants as corrosion inhibitors, in low toxicity, low residue and has prominent superiority, subsequent processing is one of the important direction of current research green corrosion inhibitors [6].

Ginkgo biloba, originating from China, was first introduced to Europe in the 18th century, and now distributes all

*Corresponding author.

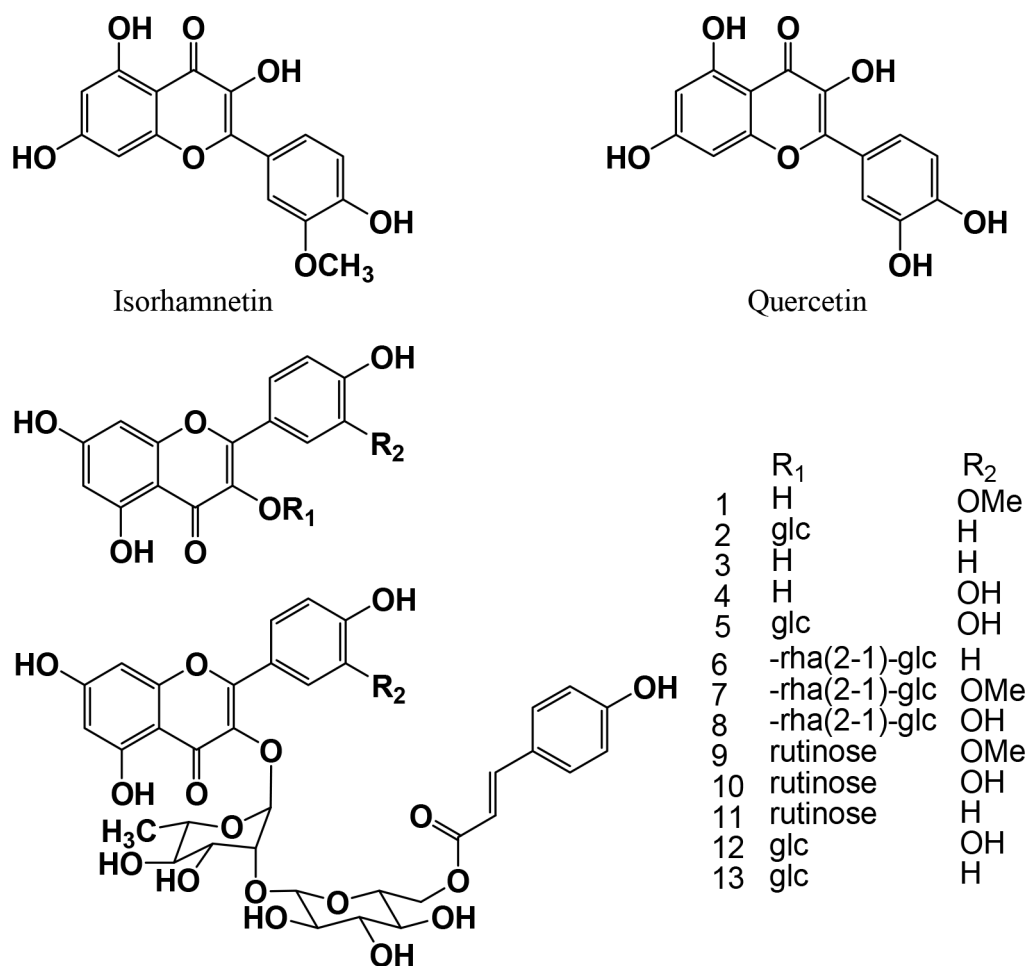


Fig. 1. Structures of flavonoids found in *Ginkgo biloba*.

over the world. Many compounds have been found in *Ginkgo biloba* leaves extracts, such as flavonoids (Fig. 1) and ginkgo lactones. Isorhamnetin, quercetin and kaempferol were the main constituents of flavonoids [6,7]. Recently, the use of *Ginkgo biloba* leaf extract as nutraceutical is becoming increasingly common, and the cytotoxicity, genotoxicity and gene expression changes elicited by exposure of human hepatic cells to *Ginkgo biloba* leaf extract was investigated for the further use [8]. Because of the multi-phenolic hydroxyl group structure, which has strong trend to bond with Fe atoms, it is suggested that *Ginkgo biloba* leaves extract (GLE) is an effective corrosion inhibitor, and in fact it displays good property against the acidic corrosion [6], but it was found in our experiment that the GLE tends to ferment in atmosphere without any modification. The target of this present work is to investigate the modified *Ginkgo biloba* leaves extract as eco-friendly acidic and microbial corrosion inhibitors.

2. Experimental

2.1. Materials

The corrosion tests were performed on N80 steel with a composition (in wt.%) C: 0.20, P: 0.015, Si: 1.45, S: 0.15, Mn:

0.020, and Fe balance. A small hole of about 3 mm diameter near the upper edge of the coupons was made to help hold them with cotton cords and suspend them into the corrosive medium. Before all measurements, the steel samples were mechanically abraded with increasing grades of emery papers (100, 600 and 1000 grit size) to remove rust particles. The treated coupons were then rinsed by petroleum ether, decreased by ethanol and dried in air. Finally, the length, width, thickness and hole diameter of the coupons were measured with a vernier caliper and the coupons were kept in moisture-free desiccators before their immersion in experimental solution. The weights of the specimens were noted before immersion. Each test run was repeated three times or three specimens were used for an experiment to check repeatability and the maximum errors of the product distribution fell within a reasonable range of $\pm 2.0\%$. Only the average data were reported hereinafter.

2.2. Inhibitors

Fresh *Ginkgo biloba* leaves were gathered in October 2013 in the campus of Xi'an Shiyou University, cleaned with water and dried in an oven at 60°C, and then were shattered into powder. The powder was refluxed with water for

4 h, and finally a light yellow aqueous extract was filtered to yield *Ginkgo biloba* leaves extract (GLE) after removed the solvent by rotary evaporation. Modified *Ginkgo biloba* leaves extract (MGLE) was prepared using GLE as raw material through Mannich reaction. The synthesis of these organic compounds was carried out according to the following procedure.

To a certain amount of GLE solution in flask, amine was added drop wise with stirring, then the thermometer, condenser pipe and blender were installed, and a certain quantity formaldehyde solution was added at last. The reaction mixture was heated to reflux for 3–4 h. The possible reaction and the modified structures of GLE are shown in Fig. 2. The reactants and the name of the products are listed in Table 1. The extract and the modified extract were obtained by the evaporation of the solution, and were used for FTIR analysis.

2.3. FTIR

FTIR spectra were recorded in KBr pellets with a Bruker Tensor 37 spectrometer in the 400–4,000 cm^{-1} region. FTIR spectrometer was calibrated by 1.5 mil and 55 micron thick polystyrene (PIKE Technologies) as reference standard before the analysis.

2.3.1. Weight loss determination

The corrosive medium for the study was hydrochloric acid solution of concentrations of 5%. It was prepared from analytical grade 38% HCl and double-distilled water. In each experiment, 250 mL acid solution was used and all corrosion experiments were performed under normal atmospheric pressure. Gravimetric measurements are carried out in a glass bottle. Each test was done with two specimens at the same time to guarantee the reliability of the results. In the weight loss experiment, Inhibitor efficiency was determined by hanging 2 pieces of the steel coupons into 250 mL 5% HCl with and without the addition of different concentrations (from 100 to 2000 ppm) of the synthesized inhibitors. After 2 h of immersion, the coupons were removed, scrubbed with bristle brush under running water in order to remove the corrosion product, washed with acetone, degreased by ethanol, dried and reweighed. Then the tests were repeated with different concentrations of inhibitors at varying temperatures (30–60°C). From the initial and final weights of the specimens, the loss of weights was calculated, and the corrosion rate of N80 steel was determined using the relation [8–10]:

$$V_i = \frac{(10^6 \Delta m)}{(A_i \cdot \Delta t)} \quad (1)$$

where V_i is the corrosion rate of a single specimen, Δt is reaction time, Δm is the mass loss of specimens corrosion and A_i is specimen surface area.

The percentage inhibition efficiency (IE (%)) was calculated using the relationship below [9]:

$$IE(\%) = \left(\frac{W_{corr} - W_{corr(inh)}}{W_{corr}} \right) \times 100 \quad (2)$$

where W_{corr} and $W_{corr(inh)}$ are the corrosion rates of mild steel in the absence and presence of inhibitors, respectively.

2.3.2. Electrochemical measurements [5–6]

The electrodes were mechanically abraded with a series of emery papers (800 and 1200 grades), then rinsed in acetone and double-distilled water before their immersion in the experimental solution. Electrochemical measurements were conducted in a conventional three-electrode thermostated cell. The electrode was inserted into a Teflon tube and isolated with polyester so that only its section (0.5 cm^2) was allowed to contact the aggressive solutions. A platinum disk as counter electrode and standard calomel electrode (SCE) as the reference electrode have been used in the electrochemical studies.

The potentiodynamic curves were recorded using a CS 350 system connected to a personal computer. The working electrode was first immersed in the test solution for 60 min to establish a steady state open circuit potential. After measuring the open circuit, potentiodynamic polarization curves were obtained with a scan rate of 0.5 mV/s. Corrosion rates (corrosion current densities) were obtained from the polarization curves by linear extrapolation of the anodic and cathodic branches of the Tafel plots at points 100 mV more positive and more negative than the E_{corr} .

Table 1
The reaction of *Ginkgo biloba* extracts and different reagents

Amine	R ₁	R ₂	Product	Solubility
Diethanolamine	C ₂ H ₄ OH	C ₂ H ₄ OH	MGLE1	Water
Morpholine	(CH ₂ CH ₂) ₂ O	(CH ₂ CH ₂) ₂ O	MGLE2	Water
Piperazine	(CH ₂ CH ₂) ₂ N	(CH ₂ CH ₂) ₂ N	MGLE3	Water

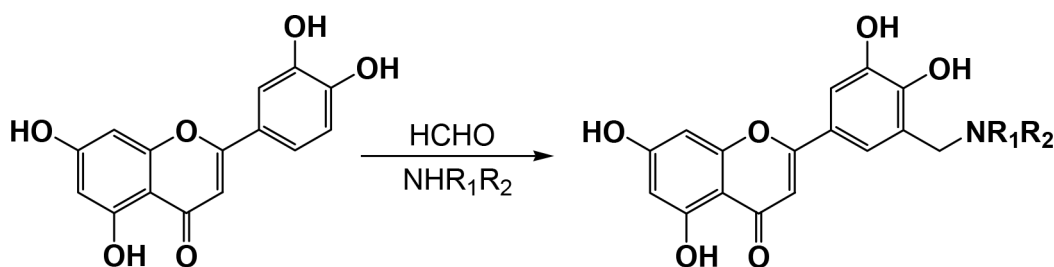


Fig. 2. The Mannich reaction of *Ginkgo biloba* flavonoid.

2.3.4. Scanning electron microscopy (SEM)[10–11]

The surface morphology of the sample under study in the absence and presence of inhibitors were investigated using a Digital Microscope Imaging scanning electron microscope (model SU6600, serial no. HI-2102-0003) at accelerating voltage of 20.0 kV. Samples were attached on the top of an aluminum stopper by means of carbon conductive adhesive tape. All micro graphs of the specimen were taken at 5009 magnification.

2.3.5. Microbiological monitoring [12,13]

Viable counts of SRB, TGB and IB were determined according to the Standard of Petroleum and Natural Gas Industry of People's Republic of China SY/T 5890-1993 (The national method of the bactericidal agent's performance), and there is a set of experimental controls in a sterilized environment without the biological species. The produced water containing the three kinds of bacteria was gathered from Xingzichuan Oilfield Factory, Yanchang Oilfield.

3. Results and discussion

3.1. FTIR analysis

Fig. 3 shows the FTIR spectra of GLE and MGLE2. The FT-IR spectra of GLE displays broad band around 3427 cm^{-1} , which corresponds to the O-H stretching vibration of the hydroxyl and/or carboxyl groups. The peaks around 2925 cm^{-1} are due to the sp^3 hybridized C-H stretching

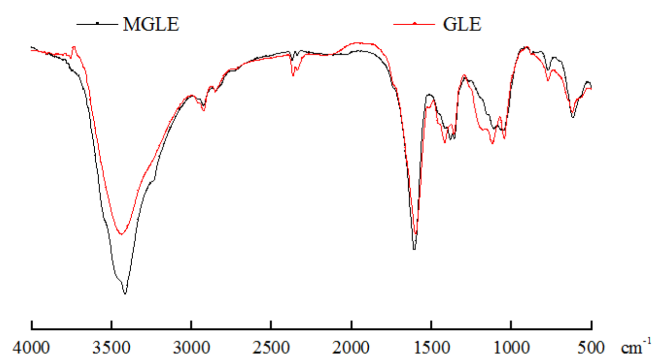


Fig. 3. FTIR of GLE and MGLE2.

vibration of alkyl groups. The peaks around 1608 cm^{-1} are associated with the skeleton vibrations of benzene and other C=O bonds. In the FTIR spectra of MGLE2, the wide and strong absorption peak around 3416 cm^{-1} is O-H stretching vibration of the hydroxyl and/or carboxyl groups, which is obviously stronger than that of GLE, indicating the increasing amount of hydroxyl after modification. The stronger peaks around 2925 cm^{-1} of MGLE2 are due to the increased methene group or other kinds of sp^3 hybridized C-H bonds.

3.2. Storage of MGLEs

From Fig. 4, it can be seen that the status of *Ginkgo biloba* extract before and after being modified after stored for a week. For GLE, the mould grew obviously, which indicates the GLE is hard to apply industrially for the bad storage. Mold is a result of various fungous' growth, causing decay of organic matter. The reason may be attributed to the carbohydrates in the extraction, and the GLE solution can provide the three main factors that could cause mold growing, moisture content, moderate temperature and the presence of oxygen [14]. Fig. 4 also shows that the modification can overcome this disadvantage significantly which will be important in the production and storage in the natural products. By the modification, the flavonoids were functioned with Mannich base groups, which have been reported with anti bacterial activities. As a result, the modified GLE solutions display a relative stable status.

3.3. Gravimetric measurements

Corrosion inhibition of GLE and MGLEs against the corrosion of N80 steel in 5% HCl solution was investigated at 303 K. Table 2 summarizes the values of inhibition efficiency (IE) from the weight-loss measurements.

The data in Table 2 clearly reveals that the IE increases as the concentration of inhibitors increases, and when the concentration reached to 1000 ppm, IE (%) of GBE, MGLE1, MGLE2 and MGLE3 reached to high values of 68.33, 64.25, 79.15 and 69.23 in 5% HCl solutions, respectively at 303K, whereas it decreased in the following order: MGLE2 > MGLE3 > GLE > MGLE1. All four inhibitors inhibited corrosion of mild steel in 5% HCl, among which MGLE2 is the best. This is due to the fact that adsorption of the inhibitor on the N80 steel increases with the inhibitor concentration, thus the mild steel surface gets efficiently protected from the medium.

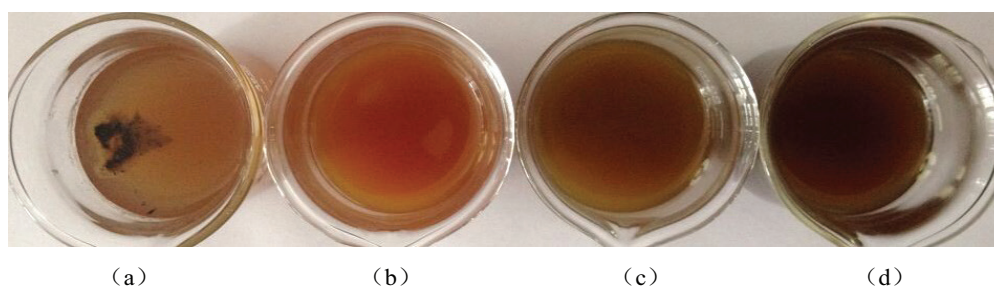


Fig. 4. Photographs of GLE and MGLEs after one week storage (a) solution of GLE, (b) solution of MGLE1, (c) solution of MGLE2, (d) solution of MGLE3.

3.3.1. Effect of temperature

Temperature is an important condition in the study of metal corrosion. In order to investigate the effect of temperature on the anti corrosion property of the inhibitors in 5% HCl solutions, weight-loss measurements were conducted over the temperature range of 303–333K in presence of different inhibitors concentrations. The correlativity between temperature and inhibition efficiency are shown in Table 3.

From Table 3, the corrosion inhibition efficiency of GLE and MGLEs against the corrosion of N80 steel in 5% HCl solution increased first and then decreased with the rising of temperature. It may be due to the fact that the low temperature will lead low reaction speed, but higher temperature accelerates hot movement of the organic molecules and

weakens the adsorption capacity of inhibitor on the metal surface.

3.3.2. Mechanism of corrosion inhibition and adsorption isotherm

It is well known that organic inhibitors establish inhibition by adsorption onto the metal surface, and the adsorption of the organic compounds can be described by two main types of interaction: physical adsorption and chemisorption, which are influenced by the nature and charge of the metal, the chemical structure of the inhibitor and the type of electrolyte.

The presence of N, O, S atoms and conjugated double bonds in the organic molecules makes the formation of p–d bonds resulting from overlap of p-electrons to the 3d vacant orbital of iron atoms, which enhances the adsorption of the inhibitors on the metal surface. Generally, organic inhibitors may be absorbed on the metal surface in one or more of the following ways [6]:

- Electrostatic interaction between the charged molecules and the charged metal;
- Interaction of unshared electron pairs in the molecules with the metal;
- Interaction of p-electrons with the metal;
- A combination of the above types.

But owing to the complex nature of adsorption and inhibition of an extract of natural product, it is impos-

Table 2
Inhibition efficiency of GLE and MGLEs against the corrosion of N80 steel in 5% HCl solution

Con (ppm)	Inhibition efficiency (IE%)			
	GLE	MGLE1	MGLE2	MGLE3
10	15.54	24.83	57.19	39.40
50	40.85	33.23	58.14	56.94
100	52.02	39.69	59.58	59.42
200	55.67	40.99	64.24	61.49
500	63.06	54.59	65.20	67.19
1000	68.85	64.25	79.15	69.23

Table 3
Inhibition efficiency of GLE and MGLEs against the corrosion of N80 steel in 5% HCl solution at different temperatures

Inh.	Temp (K)	Inhibition efficiency (%)					
		10 mg/L	50 mg/L	100 mg/L	200 mg/L	500 mg/L	1000 mg/L
GLE	303	15.54	40.85	52.02	55.67	63.06	69.85
	313	45.11	50.61	68.68	75.08	82.55	85.72
	318	59.11	66.41	78.68	85.10	89.50	91.72
	323	32.22	44.52	64.65	78.10	83.36	87.79
	333	24.16	26.88	62.46	76.72	78.49	86.47
MGLE1	303	24.83	33.23	39.69	40.99	54.59	64.25
	313	50.72	55.94	59.32	65.49	70.28	74.37
	318	60.77	65.91	79.82	83.49	88.64	90.88
	323	48.56	59.71	65.12	75.45	84.64	88.88
	333	46.48	57.72	63.88	73.96	81.37	86.12
MGLE2	303	57.19	58.14	59.58	64.24	65.20	79.15
	313	60.46	65.93	76.46	78.53	78.75	83.45
	318	65.47	79.96	81.57	87.24	92.75	93.60
	323	55.46	61.84	71.55	78.91	79.75	88.62
	333	33.88	60.64	68.22	77.45	78.89	87.88
MGLE3	303	39.40	52.94	60.42	61.49	67.19	69.00
	313	42.15	64.23	69.39	71.03	83.62	86.48
	318	65.29	70.29	76.38	85.01	90.64	92.19
	323	49.29	70.13	74.36	84.01	89.34	91.49
	333	47.89	69.12	73.08	83.44	88.09	90.06

sible for single adsorption mode between inhibitor and metal surface. The structures of phenols in *Ginkgo biloba* leave are shown in Fig. 1, and the steady conformation of Quercetin and isorhamnetin in are expressed in Fig. 5, which were simulated by a minimize energy of MM2 in Chem 3D, and the *p*-electrons of the hydroxyl groups and ether groups were colored in pink. The inhibition efficiency afforded by Mannich bases transformed from *Ginkgo biloba* leave may be attributed to the presence of electron rich phenol groups and aromatic rings. The possible absorption centers are unshared electron pair of heteroatoms and/or *p*-electrons of aromatic ring. Fig.6 shows the different modes of a Mannich base's adsorption on metal, in which there are three kinds of adsorption from O, N atoms and phenyl groups.

The interactions between inhibitor and metal surface can be examined by the adsorption isotherm. Attempts were made to correlate the degree of surface coverage values (θ) as a function of the concentration of the inhibitor (C) to various types of adsorption isotherm. Thus, the θ values, at different inhibitor concentrations in 5% HCl was evaluated from weight loss measurements ($\theta = \text{IE} (\%) / 100$) in the temperature range of 303–333 K and tested graphically for fitting to a suitable adsorption isotherm.

It was determined that the Langmuir adsorption isotherm as described by Eq. (3) [15], fitted the experimental data, which gives a straight line graph on a plot of C/θ vs. C , and the adsorption isotherm is shown in Fig. 7.

$$\frac{C}{\theta} = \frac{1}{K_{ads}} + C \quad (3)$$

where K_{ads} is the equilibrium constant of the adsorption process.

3.3.3. Thermodynamics calculations

The values of thermodynamic parameters for the adsorption of inhibitors can provide valuable information about the mechanism of corrosion inhibition. The value of K_{ads} is related to the standard free energy of adsorption, ΔG_{ads}° , by Eq. (4) [16]. Other thermodynamic parameters such as the entropy of activation ΔS_0 and the enthalpy of activation ΔH_0 for the corrosion of N80 steel in the acids solution in the presence of different concentrations MGLE2 were calculated using Eqs. (5), (6) [16], and are listed in Table 4.

$$K_{ads} = \frac{1}{55.5} \exp\left(\frac{-\Delta G_{ads}^{\circ}}{RT}\right) \quad (4)$$

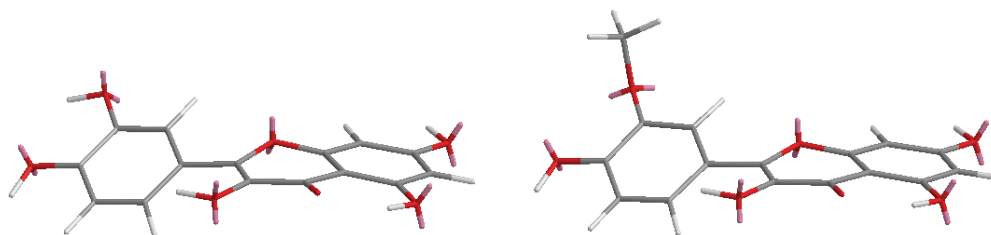


Fig. 5. The steady conformation of Quercetin and isorhamnetin.

where R is the universal gas constant and T is the absolute temperature. The value of 55.5 is the molar concentration of water in solution expressed in mg/L.

$$\ln K = \frac{-\Delta H_0}{RT} + \text{constant} \quad (5)$$

$$\Delta S_0 = \frac{(\Delta H_0 - \Delta G_0)}{T} \quad (6)$$

where ΔH_0 and ΔS_0 are the adsorption enthalpy and entropy respectively.

From Table 4, the negative value of ΔG_{ads}° indicates spontaneous adsorption of MGLE2 molecules on the steel

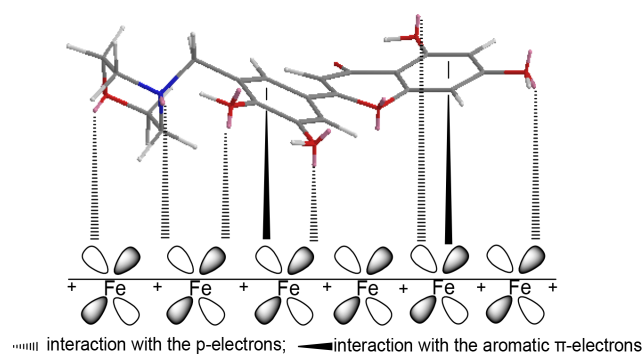


Fig. 6. The absorption of Mannich base (MGLE2) on the steel surface by coordination.

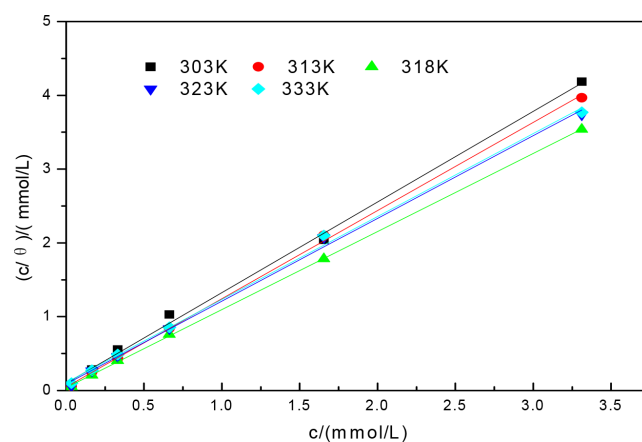


Fig. 7. Langmuir adsorption isotherm of MGLE2 on N80 steel in 0.5% HCl at different temperatures.

Table 4
Thermodynamic parameters for adsorption of MGLE2 on N80 steel in 5% HCl solutions at different temperatures from Langmuir adsorption isotherm

T/°C	ΔG_0 (kJ/mol)	ΔH_0 (kJ/mol)	ΔS_0 (J/mol·K)
30	-32.48	2.51	115.39
40	-36.29	2.51	123.88
45	-37.50	2.51	125.76
50	-35.84	2.51	118.66
60	-36.39	2.51	116.76

surface and a strong interaction between inhibitor molecules and metal surface. Generally, values of ΔG_{ads} around $-20 \text{ kJ} \cdot \text{mol}^{-1}$ or lower are consistent with electrostatic interaction between the charged molecules and the charged metal (physisorption); those around $-40 \text{ kJ} \cdot \text{mol}^{-1}$ or higher involve charge sharing or transfer from organic molecules to the metal surface to form a co-ordinated type of bond (chemisorption) [17]. The calculated value of ΔG_{ads} is near -40 kJ/mol , indicating MGLE2 adsorbing onto steel surface by both predominantly by chemical process. The value of ΔH_0 provides further information about the mechanism of corrosion inhibition. The positive values of ΔH_0 indicate that the process of adsorption of the inhibitor on the steel surface was an endothermic process. An exothermic adsorption process may be chemisorption or physisorption or mixture of both, whereas endothermic process is attributed to chemisorption. In the present work, the positive value of ΔH_{ads} indicates that this inhibitor can be considered to adsorb by a mixture of both processes. Besides, the values of ΔS_0 in the presence of the inhibitors were large and positive. In short, the adsorption process of this study is spontaneous, endothermic and entropy increase process.

3.3.4. Potentiodynamic polarization

Polarization studies were carried out to gain information concerning the kinetics of the anodic and cathodic reactions. The potentiodynamic polarization curves for mild steel in 5% HCl acid solution in the absence and presence of various concentrations of the inhibitors are shown in Fig. 6. The values of the various electrochemical parameters such as corrosion potential (E_{corr}), cathodic and anodic Tafel slopes (b_a , b_c), and corrosion current density I_{corr} derived from Tafel polarization for all the inhibitor concentrations are given in Table 5. The IE was calculated using the following equation:

$$IE(\%) = \left(\frac{I_{\text{corr}} - I_{\text{corr(inh)}}}{I_{\text{corr}}} \right) \times 100 \quad (7)$$

Here, I_{corr} and $I_{\text{corr(inh)}}$ are the corrosion current densities (mA/cm^2) in the absence and presence of the inhibitor, respectively. It is clear from Fig. 8 that the presence of MGLE2 decreases cathodic and anodic slopes with the increasing inhibitor concentration. Moreover, inspection of Table 5 reveals that the values of b_c change slightly in the presence of MGLE2, whereas more pronounced change occurs in the values of b_a , indicating that both the anodic and

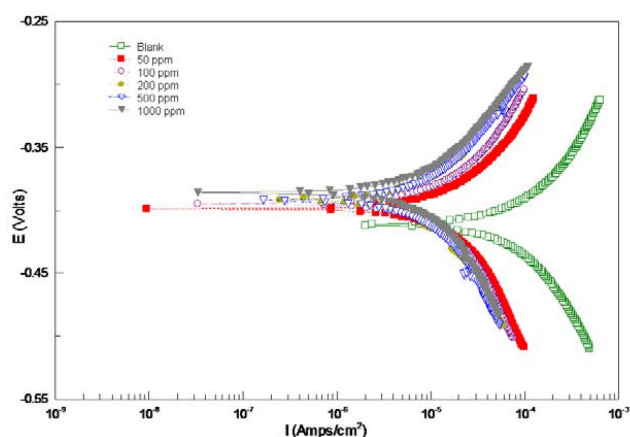


Fig. 8 Typical polarization curves for corrosion of N80 steel in 5% HCl in the absence and presence of different concentrations of MGLE2.

cathodic reactions are affected, but the effect on the anodic reactions is more prominent. Thus, MGLE2 acts as a mixed-type, but predominantly anodic, inhibitor. Meanwhile, it is evident that I_{corr} decreases significantly with increasing concentration of MGLE2. This is because of increase in the blocked fraction of the metal surface by adsorption. Further, the concentration of MGLE2 has less effect on the E_{corr} , which indicates that MGLE2 acts as a mixed type of inhibitor. The inhibition efficiencies obtained from potentiodynamic polarization are different from those calculated from weight-loss measurements; which may be because the weight-loss method gives average corrosion rate, whereas the electrochemical method gives instantaneous corrosion rates. These variations may also arise because of the different times required to form the adsorbed layers of the inhibitors on the metal surface that inhibit corrosion [18–20].

3.4. Scanning electron microscopy

In order to evaluate the conditions of the steel surfaces in contact with 5% HCl acid solutions, SEM was carried out. Fig. 9a shows a SEM image of the polished steel sample. Fig. 9b shows a SEM image of the surface of the steel specimens after immersion in 5% HCl solution media without inhibitor molecules for 12 h. This micrograph shows the result of cracks caused by corrosion attack due to exposure of steel into 5% HCl solution. Fig. 9c shows the image of the surface of the steel specimens immersed for 12 h in 5% HCl solutions containing 500 mg/L MGLE2 at 318 K. As can be seen from Fig. 9c, the surface was free from pits and appeared smooth, and only small points and groove were found on the surface, which is much less damaged than that without any corrosion inhibitors. This was due to strong adsorption of MGLE2 on the steel surface, which accords with the mechanism analysis above.

3.5. Antibacterial activity against oil field microorganism

Corrosion is an electrochemical process leading to the deterioration of materials that can be caused or accelerated by microbiological activity, so called Micro biologically

Table 5

Potential dynamic polarization data for corrosion of N80 steel in 5% HCl in the absence and presence of different concentrations of the MGLE2

Concentration ppm	$-E_{\text{corr}}$ (mV)	I_{corr} $\mu\text{A}/\text{cm}^2$	b_a mV/dec	b_c mV/dec	CR mm/a	IE %
blank	0.53313	368.12	269.08	193.63	4.3286	–
50	0.53069	291.33	242.17	174.52	3.4269	20.86
100	0.52254	254.83	225.69	139.21	2.7264	30.78
200	0.51176	221.81	176.02	124.05	2.3076	39.75
500	0.45260	181.74	104.27	112.57	1.9314	50.63
1,000	0.43228	145.26	84.31	106.71	1.4281	60.54

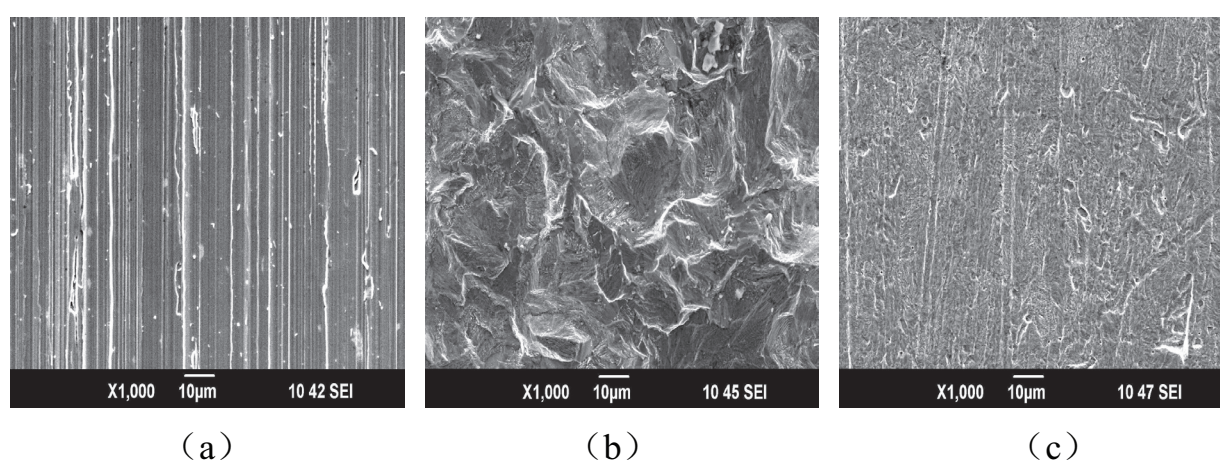


Fig. 9 SEM micro graphs of steel samples after 12 h immersion period (a) polished surface, (b) after 12 h immersion in 5% HCl, (c) after 12 h immersion in 5% HCl + 500 mg/L MGLE2.

Influenced Corrosion (MIC). It is estimated that 30–50% of the corrosion cases are a result of microbial activity. The MIC is mainly caused by the growth of such oil field microorganism as sulfate reducing bacteria (SRB), iron bacteria (IB) and total general bacteria (TGB) in oil pipelines, which is considered as a major problem for water treatment in the oil field. MIC can result in different types of attack, such as pitting, crevices, dealloying and erosion in pipelines. In addition, microbial degradation of crude oil can lead to increased acidity in the oil phase, and the high acid-contained oil is a problem concerning corrosion of pipelines. Even more serious, the interaction of IB, SRB and TGB can accelerate the corrosion rate, in other word, the corrosion in the mixture of IB, SRB and TGB was more serious than in a single microbial system. Based on this case, different treatment system to inhibit corrosion should be considered, among which using bactericide has received the greatest acceptance. Currently, oxidizer, aldehyde, quaternary ammonium salt and heterocycle compounds, such as Cl_2 , ClO_2 , formaldehyde, pentane-1,5-dial, trichloroisocyanuric acid (TCCA) and ect., have been used as bactericides, but the toxicity and oxidation tests have been conducted on a limited selection [6,12].

Since the structures of the main composition in *Ginkgo biloba* have been determined as shown in Fig. 1, and the flavonoids have been found to incline to combine with pro-

Table 6

The antibacterial activity of MGLE against oilfield water-born bacteria

MGLEs	Concentration	Microbiotic Concentration /mL		
	mg/L	SRB	IB	TGB
–	–	110.0	110.0	110.0
MGLE	1,000	2.0	2.0	2.0
	500	2.0	6.0	20.0
MGLE1	1,000	20.0	2.0	2.0
	500	77.0	2.0	20.0
MGLE2	1,000	2.0	1.3	6.0
	500	2.0	6.0	25.0
MGLE3	1,000	1.3	0.0	2.0
	500	2.0	2.0	25.0

teins and shown some antibacterial activities, the MGLEs are anticipated to be bactericides for oil field microorganism. In the following work, the antifungal activity of these extracts against oil field microorganism was tested under the concentrations of 1,000 mg/L and 500 mg/L, and the results are summarized in Table 6. The table shows that the

MGLEs as well as GLE are active against the three microorganisms under the concentration of 1000 mg/L, except the MGLE1 for SRB. As the concentration reduced to 500 mg/L, the inhibitions are still potent in most of the cases with slightly higher micro biotic concentrations. But the inhibition of MGLE1 for SRB depresses obviously.

4. Conclusion

Base on the natural product, the extract and its derivatives of *Ginkgo biloba* leave (GLE and MGLEs, respectively), at concentrations in the range 10 to 1,000 ppm, act as moderate to highly effective green and eco-friendly inhibitors of corrosion of steel in 5% HCl by forming protective layer, and they absorbed on the mild steel surface according to Langmuir adsorption isotherm. The best inhibition efficiency, 93.6%, was achieved by use of 1,000 ppm MGLE2. The inhibition efficiency increases first and then decreased with the rise in temperature in the inhibited solution. Electrochemical polarization study revealed that the *Ginkgo biloba* leaves extract acts as mixed-type, but predominantly anodic, inhibitor. Then SEM morphology revealed the formation of a protective film type of inhibitor by reducing both anodic and cathodic current densities. All the results obtained from polarization, SEM and weight loss are in good agreement with each other. In addition, the MGLEs as well as GLE are active against sulfate reducing bacteria (SRB), iron bacteria (IB) and total general bacteria (TGB), except the MGLE1 for SRB.

Acknowledgement

This work was financially supported by the grants from National Science Foundation of China (51504193) and State Key Laboratory of Petroleum Pollution Control.

References

- [1] A.A.P. Sidharth, Effect of pitting corrosion on ultimate strength and buckling strength of plates—a review, *Dig. J. Nano mater. Bios.*, 4 (2009) 783–788.
- [2] Y.F. Yang, X.T. Zhao, G.M. Qiu, Development status of acidization corrosion inhibitor in China, *Corros. Prot. Petrochem. Ind.*, 24 (2001) 6–9.
- [3] S.J. Li, H.J. Yu, J.G. Wang, Synthesis and performance properties of compounded Mannich base corrosion inhibitor for hydrochloric acidizing fluids, *Oilfield. Chem.*, 25 (2008) 118–121.
- [4] Y. Zhang, Y. Lu, Y. Zhang, Study on the synthesis and performance of a Mannich based acidization corrosion inhibitor, *Oilfield. Chem.*, 30 (2013) 111–114.
- [5] G. Chen, M. Zhang, M. Pang, Extracts of *Punica granatum* Linne husk as green and eco-friendly corrosion inhibitors for mild steel in oil fields, *Res. Chem. Intermed.*, 39 (2013) 3545–3552.
- [6] G. Chen, M. Zhang, J.R. Zhao, Investigation of *Ginkgo biloba* leave extracts as corrosion and Oil field microorganism inhibitors, *Chem. Cent. J.*, 7 (2013) 1–7.
- [7] M.G. Grollino, G. Raschella, E. Cordelli, P. Villani, M. Pieraccioli, I. Paximadas, S. Malandrino, S. Bonassio, F. Pacchierotti, Cytotoxicity, genotoxicity and gene expression changes elicited by exposure of human hepatic cells to *Ginkgo biloba* leaf extract, *Food Chem. Toxicol.*, 109 (2017) 486–496.
- [8] X.J. Su, G.A. Shen, S.K. Di, R.A. Dixon, Y.Z. Pang, Characterization of UGT716A1 as a multi-substrate UDP: Flavonoid glucosyl transferase gene in *Ginkgo biloba*, *Front Plant Sci.*, 8 (2017) 2085.
- [9] I.B. Obot, N.O. Obi-Egbedi, N.W. Odozi, Acenaphtho [1,2-b] quinoxaline as a novel corrosion inhibitor for mild steel in 0.5 M H₂SO₄, *Corros. Sci.*, 52 (2010) 923–926.
- [10] P. Mohan, R. Usha, G.P. Kalaignan, Inhibition effect of benzohydrazide derivatives on corrosion behaviour of mild steel in 1M HCl, *J. Chem.*, 23 (2013) 1–7.
- [11] M.M. Fares, A.K. Maayta, M.M. Al-Qudah, Pectin as promising green corrosion inhibitor of aluminum in hydrochloric acid solution, *Corros. Sci.*, 60 (2012) 112–117.
- [12] G. Chen, Q.L. Gao, F.Y. Ma, Research of the corrosion inhibition and inhibition to oilfield bacteria by persimmon husk extraction, *Chem. Eng. Oil. & Gas.*, 42 (2013) 515–519.
- [13] G. Chen, M. Pang, Y.J. Mo, Application of pomegranate husk extract in the treatment of oilfield produced water, *Chem. Eng. Oil. & Gas.*, 42 (2013) 83–85.
- [14] S.A. Ali, H.A. Al-Muallem, S.U. Rahman, Bis-isoxazolidines: A new class of corrosion inhibitors of mild steel in acidic media, *Corros. Sci.*, 50 (2008) 3070–3077.
- [15] S.S. Shivapura, N.S.M. Kikkeri, Ziziphus mauritiana leaves extracts as corrosion inhibitor for mild steel in H₂SO₄ and HCl solutions, *Eur. J. Chem.*, 3 (2012) 426–432.
- [16] X.H. Li, G.N. Mu, Tween-40 as corrosion inhibitor for cold rolled steel in sulphuric acid: weight loss study, electrochemical characterization and AFM, *Appl. Surf. Sci.*, 252 (2005) 1254–1265.
- [17] X.H. Li, S.D. Deng, H. Fu, Inhibition action of allyl thiourea for steel in H₂SO₄ solution, *Corros. & Prot.*, 32 (2011) 958–961.
- [18] A.S. Fouda, S.A. EL-Sayyad, N-3-hydroxyl-2-naphthoyl hydrazone derivatives as inhibitors for corrosion of carbon steel in H₂SO₄ acid solution, *Anti-Corros. Method. M.*, 58 (2011) 63–69.
- [19] G.N. Mu, X.H. Li, Q. Qu, Molybdate and tungstate as corrosion inhibitors for cold rolling steel in hydrochloric acid solution, *Corros. Sci.*, 48 (2006) 445–459.
- [20] M.G. Hosseini, M. Ehteshamzadeh, T. Shahrabi, Protection of mild steel corrosion with Schiff bases in 0.5M H₂SO₄ solution, *Electrochim. Acta.*, 52 (2007) 3680–3685.